

## Similarity of nuclear structure in the $^{132}\text{Sn}$ and $^{208}\text{Pb}$ regions: Proton-neutron multiplets

L. Coraggio,<sup>1</sup> A. Covello,<sup>1,2</sup> A. Gargano,<sup>1</sup> and N. Itaco<sup>1,2</sup>

<sup>1</sup>*Istituto Nazionale di Fisica Nucleare, Complesso Universitario di Monte S. Angelo, I-80126 Napoli, Italy*

<sup>2</sup>*Dipartimento di Scienze Fisiche, Università di Napoli Federico II, Complesso Universitario di Monte S. Angelo, I-80126 Napoli, Italy*

(Received 22 January 2009; published 27 August 2009)

Starting from the striking similarity of proton-neutron multiplets in  $^{134}\text{Sb}$  and  $^{210}\text{Bi}$ , we perform a shell-model study of nuclei with two additional protons or neutrons to find out to what extent this analogy persists. We employ effective interactions derived from the CD-Bonn nucleon-nucleon potential renormalized by use of the  $V_{\text{low-k}}$  approach. The calculated results for  $^{136}\text{Sb}$ ,  $^{212}\text{Bi}$ ,  $^{136}\text{I}$ , and  $^{212}\text{At}$  are in very good agreement with the available experimental data. The similarity between  $^{132}\text{Sn}$  and  $^{208}\text{Pb}$  regions is discussed in connection with the effective interaction, emphasizing the role of core polarization effects.

DOI: [10.1103/PhysRevC.80.021305](https://doi.org/10.1103/PhysRevC.80.021305)

PACS number(s): 21.60.Cs, 21.30.Fe, 27.60.+j, 27.80.+w

Since its advent more than 50 years ago, the shell model has been the basic framework for understanding the structure of complex nuclei in terms of individual nucleons. Within this model, nuclei around doubly closed shells play a special role. In fact, they yield direct information on the two basic ingredients of the model: single-particle (SP) energies and matrix elements of the effective interaction. This makes them the best testing ground for realistic shell-model calculations where the effective interaction is derived from the free nucleon-nucleon ( $NN$ ) potential.

For a long time our knowledge of nuclei with few-valence particles or holes has been mostly limited to neighbors of stable or long-lived doubly magic  $^{16}\text{O}$ ,  $^{40}\text{Ca}$ ,  $^{48}\text{Ca}$ ,  $^{56}\text{Ni}$ , and  $^{208}\text{Pb}$ . However, during the past decade there has been substantial progress in the experimental study of nuclei far from the stability line, and the development of radioactive nuclear beams is currently giving strong impetus to the study of exotic nuclei around  $^{78}\text{Ni}$ ,  $^{100}\text{Sn}$ , and  $^{132}\text{Sn}$ . These new data pose challenging questions about the evolution of the shell structure, as for instance the validity of magic numbers when moving far away from stability and the existence of possible changes in the mean field as well as in the two-body interaction [1–3].

In this context, nuclei “northeast” of  $^{132}\text{Sn}$  are of special interest, because in recent experiments some peculiar properties have been observed that might be interpreted as the onset of a shell-structure modification (see introductory discussion in Ref. [4]). To investigate whether these features really depend on the exoticism of  $^{132}\text{Sn}$  neighbors, we believe that a comparative study of their spectroscopic properties and those of nuclei close to stable  $^{208}\text{Pb}$  is desirable.

As is well known,  $^{132}\text{Sn}$  and  $^{208}\text{Pb}$ , which are very differently located with respect to the valley of stability, both exhibit a strong neutron-proton asymmetry and strong shell closures. The existence of a specific resemblance between  $^{132}\text{Sn}$  and  $^{208}\text{Pb}$  regions was pointed out long ago in Ref. [5], where it was noticed that every SP proton or neutron state in the  $^{132}\text{Sn}$  region, characterized by quantum numbers ( $nlj$ ), has its counterpart around  $^{208}\text{Pb}$  with quantum numbers ( $nl + 1j + 1$ ). Based on this resemblance, the discrepancies between experimental and Woods-Saxon SP energies in  $^{208}\text{Pb}$

region were then used to correct the SP energies calculated for  $^{132}\text{Sn}$  region, so as to predict the energies of unobserved states. A few years later, an analysis similar in spirit to that of Ref. [5] was carried out in Ref. [6] using SP energies calculated with three different independent-particle models.

Until recent years, however, the data available for nuclei around  $^{132}\text{Sn}$  have not been sufficient to clearly assess the similarity of the spectroscopy of  $^{132}\text{Sn}$  and  $^{208}\text{Pb}$  regions. However, in several recent articles this similarity has been exploited to interpret new observed levels in  $^{132}\text{Sn}$  neighbors (see for instance Refs. [7–11]). In this regard, it is of key importance the fact that, given the correspondence between the SP levels, the matrix elements of the effective interactions in  $^{132}\text{Sn}$  and  $^{208}\text{Pb}$  regions are expected to be proportional to one another. This has stimulated several shell-model calculations on nuclei around  $^{132}\text{Sn}$  [12–14] with two-body effective interactions originating from the modified version [15] of the Kuo-Herling interaction [16], originally designed for the Pb region. However, these attempts have not been successful, as discussed for instance in Ref. [14], where the conclusion was drawn that a consistent Hamiltonian for the three nuclei beyond the  $N = 82$  shell closure,  $^{134}\text{Sb}$ ,  $^{135}\text{Sb}$ , and  $^{134}\text{Sn}$ , had yet to be found.

In the works of Refs. [4,17,18] we have shown that the properties of these nuclei are well accounted for by a unique shell-model Hamiltonian with SP energies taken from experiment and two-body effective interaction derived from the CD-Bonn  $NN$  potential [19]. Along the same lines we have performed a calculation for  $^{210}\text{Bi}$ , obtaining results in very good agreement with experiment [20].

Based on these results, we have found it interesting to perform a comparative shell-model study of  $^{132}\text{Sn}$  and  $^{208}\text{Pb}$  regions using the same Hamiltonians as in our aforementioned studies. Here, we focus on odd-odd nuclei extending our calculations for  $^{134}\text{Sb}$  and  $^{210}\text{Bi}$  to systems with an additional pair of protons or neutrons. These are  $^{136}\text{I}$  and  $^{136}\text{Sb}$  in  $^{132}\text{Sn}$  region and their counterparts in  $^{208}\text{Pb}$  region,  $^{212}\text{At}$  and  $^{212}\text{Bi}$ . A main aim of this study is to emphasize the striking similarity between proton-neutron multiplets in  $^{134}\text{Sb}$  and  $^{210}\text{Bi}$ , which is successfully reproduced by our effective interactions, and

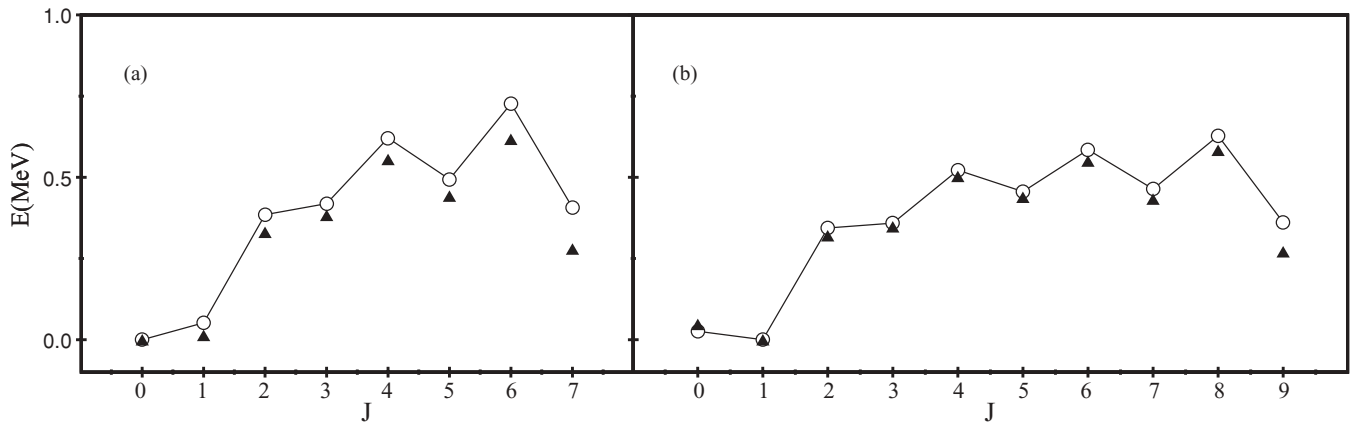


FIG. 1. (a) Proton-neutron  $\pi g_{7/2} \nu f_{7/2}$  multiplet in  $^{134}\text{Sb}$ . (b) Proton-neutron  $\pi h_{9/2} \nu g_{9/2}$  multiplet in  $^{210}\text{Bi}$ . The theoretical results are represented by open circles while the experimental data by solid triangles.

investigate to what extent these interactions predict persistence of similarity when adding two identical particles. It is worth pointing out that our effective interaction virtually accounts for excitations left out from the chosen shell-model space. We shall see that a crucial role is played by the renormalization induced by the core through one particle-one hole (1p1h) excitations.

In our shell-model calculations for  $^{132}\text{Sn}$  neighbors we assume that the valence protons occupy the five levels  $0g_{7/2}$ ,  $1d_{5/2}$ ,  $1d_{3/2}$ ,  $2s_{1/2}$ , and  $0h_{11/2}$  of the 50–82 shell, while for neutrons the model space includes the six levels  $1f_{7/2}$ ,  $2p_{3/2}$ ,  $0h_{9/2}$ ,  $2p_{1/2}$ ,  $1f_{5/2}$ , and  $0i_{13/2}$  of the 82–126 shell. Similarly, for  $^{208}\text{Pb}$  neighbors we take as model space for the valence protons the six levels of the 82–126 shell and let the valence neutrons occupy the seven levels  $1g_{9/2}$ ,  $0i_{11/2}$ ,  $0j_{15/2}$ ,  $2d_{5/2}$ ,  $3s_{1/2}$ ,  $1g_{7/2}$ , and  $2d_{3/2}$  of the 126–184 shell.

As mentioned above, for both regions the two-body effective interaction is derived from the CD-Bonn  $NN$  potential. Details on the derivation, as well as on the adopted SP proton and neutron energies, can be found in Refs. [17] and [20] for  $^{132}\text{Sn}$  and  $^{208}\text{Pb}$ , respectively. We only mention here that the short-range repulsion of the  $NN$  potential is renormalized by means of the  $V_{\text{low-k}}$  potential [21], which is then used, with the addition of the Coulomb force for protons, to derive the effective interaction  $V_{\text{eff}}$  within the framework of the  $\hat{Q}$ -box folded-diagram expansion [22]. The calculation of the  $\hat{Q}$  box is performed at second order in  $V_{\text{low-k}}$ , which from now on denotes the renormalized nuclear plus Coulomb interaction. Namely, we include four two-body terms: the  $V_{\text{low-k}}$ , the two core polarization diagrams  $V_{1\text{p}1\text{h}}$  and  $V_{2\text{p}2\text{h}}$ , corresponding to one particle-one hole and two particle-two hole excitations, and a ladder diagram accounting for excluded configurations above the chosen model space. The shell-model calculations have been performed by using the NUSHELLX code [23].

To start with, we consider  $^{134}\text{Sb}$  and  $^{210}\text{Bi}$ . We report in Fig. 1 the calculated and experimental proton-neutron mul-

tiplets in  $^{134}\text{Sb}$  arising from the  $\pi g_{7/2} \nu f_{7/2}$  configuration together with those in  $^{210}\text{Bi}$  arising from the  $\pi h_{9/2} \nu g_{9/2}$  configuration, just as they are shown in Refs. [4] and [20], respectively. This gives clear evidence of the striking similarity of the multiplets in the two nuclei. We see that in both cases a sizable energy gap exists between the  $2^-$  state and the nearly degenerate  $0^-$  and  $1^-$  states, although the ground state is  $0^-$  in  $^{134}\text{Sb}$  and  $1^-$  in  $^{210}\text{Bi}$ . As discussed in detail in Ref. [20], the measurement of the ground-state spin in  $^{210}\text{Bi}$  as  $1^-$  dates back to some 50 years ago [24] and since then the explanation of this peculiar feature has attracted great interest. For  $^{134}\text{Sb}$ , instead, the observation of the  $0^-$  and  $1^-$  states was only a recent experimental achievement [14,25]. Note that our calculations account for the position of the  $0^-$  and  $1^-$  states in both nuclei.

A common feature of the multiplets in  $^{134}\text{Sb}$  and  $^{210}\text{Bi}$  is also a distinctive energy staggering with the same magnitude and phase between the odd and even members starting from the  $3^-$  state. As a consequence, the maximum aligned states come down in energy becoming the second excited states in both nuclei, which makes them isomers.

From Fig. 1 we also see that our results are in very good agreement with experiment, as discussed in detail in Refs. [4] and [20]. This testifies to the soundness of our proton-neutron effective interactions, in particular as regards the diagonal two-body matrix elements for the  $\pi g_{7/2} \nu f_{7/2}$  and  $\pi h_{9/2} \nu g_{9/2}$  configurations. The members of the multiplets are in fact characterized by very little configuration mixing, the percentage of the leading component ranging from 100 to 88% in  $^{134}\text{Sb}$  and from 100 to 91% in  $^{210}\text{Bi}$ .

To have a better insight into the nature of our effective interactions, we have analyzed the various terms that contribute to them to find out their relative importance in determining the final values of the matrix elements. In both  $^{132}\text{Sn}$  and  $^{208}\text{Pb}$  regions, it turns out that the major contribution to produce the right  $0^- - 1^-$  spacing arises from virtual interactions with core particles induced by the  $NN$  potential, more precisely from core polarization through 1p1h excitations. To evidence the role of these excitations, in Table I we report

TABLE I. Diagonal matrix elements of  $V_{\text{low-k}}$  and  $V_{\text{1p1h}}$  (in MeV) for proton-neutron configurations in  $^{132}\text{Sn}$  and  $^{208}\text{Pb}$  regions.

$J^\pi$	$\pi 0g_{7/2} \nu 1f_{7/2}$		$\pi 0h_{9/2} \nu 1g_{9/2}$	
	$V_{\text{low-k}}$	$V_{\text{1p1h}}$	$V_{\text{low-k}}$	$V_{\text{1p1h}}$
$0^-$	-0.596	0.089	-0.468	0.049
$1^-$	-0.371	-0.079	-0.311	-0.105
$2^-$	-0.350	0.167	-0.292	0.115
$3^-$	-0.210	0.047	-0.165	0.011
$4^-$	-0.165	0.156	-0.146	0.115
$5^-$	-0.197	0.079	-0.131	0.045
$6^-$	-0.070	0.146	-0.079	0.099
$7^-$	-0.348	0.080	-0.151	0.059
$8^-$			-0.035	0.101
$9^-$			-0.274	0.059

the diagonal matrix elements of  $V_{\text{low-k}}$  and  $V_{\text{1p1h}}$  for the  $\pi g_{7/2} \nu f_{7/2}$  and  $\pi h_{9/2} \nu g_{9/2}$  configurations. We see that the 1p1h contribution substantially modifies in some cases the bare  $V_{\text{low-k}}$  interaction. In particular, it is the 1p1h term that, having opposite sign for the  $0^-$  and  $1^-$  states, brings the latter down in energy. From Table I we also see that the matrix elements of  $V_{\text{low-k}}$  as well as  $V_{\text{1p1h}}$  have practically the same behavior and weight in the two different mass regions. Finally, we may mention that not only the contribution from 1p1h excitations but also the  $V_{\text{2p2h}}$  and ladder terms go in the same direction, as shown in Refs. [4,20].

We are now going to present our results for the two counterpart pairs,  $^{136}\text{I}$ - $^{212}\text{At}$  and  $^{136}\text{Sb}$ - $^{212}\text{Bi}$ , with two more valence protons and neutrons, respectively. In Figs. 2 and 3, the calculated energies for the former and latter pair are compared with the experimental ones [26–28]. We show in Fig. 2(a) the calculated energies of  $^{136}\text{I}$  for the lowest states with  $J^\pi = 0^-$  to  $7^-$ , which are dominated by the  $(\pi g_{7/2})^3 \nu f_{7/2}$  configuration, and in Fig. 2(b) the energies of the  $J^\pi = 0^-$  to  $9^-$  states in  $^{212}\text{At}$ , arising from the  $(\pi h_{9/2})^3 \nu g_{9/2}$  configuration. In Figs. 3(a) and 3(b), we report the energies of the corresponding states in  $^{136}\text{Sb}$  and  $^{212}\text{Bi}$ , which are dominated by the  $\pi g_{7/2} (\nu f_{7/2})^3$  and  $\pi h_{9/2} (\nu g_{9/2})^3$  configurations, respectively. Note that our predictions for  $^{136}\text{Sb}$  were first reported in the

work of Ref. [28] to help interpreting some new experimental data.

For all four nuclei, the considered states receive significant contributions from configurations other than the dominant one. In fact, we find that the the percentage of the  $(\pi g_{7/2})^3 \nu f_{7/2}$  configuration for the states of  $^{136}\text{I}$  and of the  $(\pi h_{9/2})^3 \nu g_{9/2}$  configuration for the states of  $^{212}\text{At}$  ranges from 64 to 75% and from 66 to 75%, respectively. As for  $^{136}\text{Sb}$  and  $^{212}\text{Bi}$ , it turns out that the percentage of the  $\pi g_{7/2} (\nu f_{7/2})^3$  and  $\pi h_{9/2} (\nu g_{9/2})^3$  configurations goes from 58 to 76% and from 48 to 75%. Note that the configuration mixing is particularly large for  $^{212}\text{Bi}$ , the percentage of components other than the dominant one exceeding 50% for the  $0^-$  state. We shall come back to this point later.

As regards the experimental states, we have excluded those with no or multiple spin-parity assignment. This is the case of the  $7^-$  state in  $^{136}\text{I}$ , whose position is still a matter of discussion [27,29]. From Figs. 2 and 3 we see that the agreement between theory and experiment is very good, the largest discrepancy being about 80 keV for the  $9^-$  state in  $^{212}\text{At}$ . Note, however, that some experimental levels are still missing.

Although the observation of the missing states is certainly needed to further verify the outcome of our calculations, the present comparison between theory and experiment encourages use of our predictions to study how the structure of proton-neutron multiplets is affected when adding two identical particles. From this point of view, the theoretical curves of Figs. 2 and 3 may be considered the evolution of the  $\pi g_{7/2} \nu f_{7/2}$  and  $\pi h_{9/2} \nu g_{9/2}$  multiplets.

These curves all have a similar shape, but they differ from that of the multiplets in  $^{134}\text{Sb}$  and  $^{210}\text{Bi}$ . The main new features are an overall flattening of the staggering and an energy increase of the  $0^-$  state with respect to the  $1^-$  one. These are a manifestation of the dominant role played by pairing correlations, which means that the two additional protons or neutrons in both  $A = 136$  and  $212$  systems are prevalently coupled to zero angular momentum. However, the wave functions of the states reported in Figs. 2 and 3 also contain components with the pair coupled to  $J \neq 0$ , which have a larger weight when a neutron rather than a proton pair is added. As a matter of fact, it turns out that the proton-proton pairing

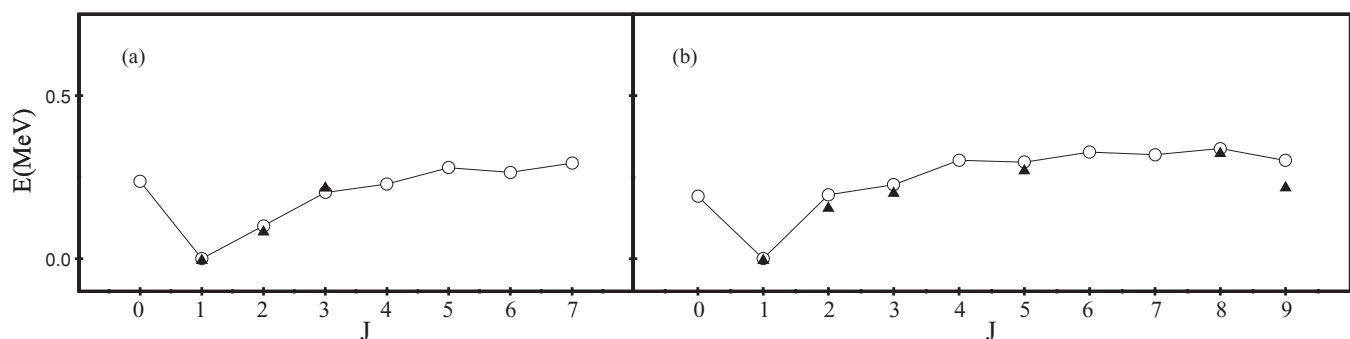
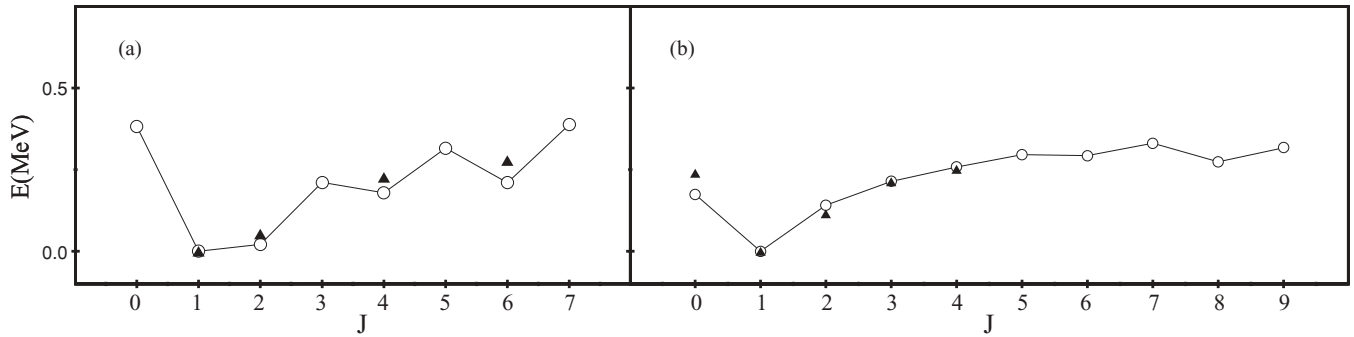


FIG. 2. Low-lying proton-neutron multiplet in  $^{136}\text{I}$  (a) and  $^{212}\text{At}$  (b). The theoretical results are represented by open circles while the experimental data by solid triangle. See text for comments.

FIG. 3. Same as Fig. 2 for  $^{136}\text{Sb}$  (a) and  $^{212}\text{Bi}$  (b).

component of our effective interaction plays a more significant role than that of the neutron-neutron one, which is largely due to the  $1p1h$  excitations. We report the diagonal matrix elements of  $V_{\text{low-k}}$  and  $V_{1p1h}$  for the  $(\pi 0g_{7/2})^2$ ,  $(\pi 0h_{9/2})^2$ ,  $(\nu 1f_{7/2})^2$ , and  $(\nu 1g_{9/2})^2$  configurations in Table II, where we see that the proton-proton pairing is essentially determined by  $V_{1p1h}$  through the large and negative values of the  $J^\pi = 0^+$  matrix elements as compared to the  $J \neq 0$  ones. This is not the case for the  $V_{1p1h}$  neutron-neutron matrix elements that are all scaled down, thus producing a non-negligible attenuation of the pairing force. Note that the differences between proton-proton and neutron-neutron interactions are also due to the Coulomb force, which, however, does not affect significantly the  $V_{1p1h}$  matrix elements. Similarly to the proton-neutron case, we see that the matrix elements shown in Table II have comparable magnitudes in  $^{132}\text{Sn}$  and  $^{208}\text{Pb}$  regions.

It is worth pointing out that our results are consistent with the experimental energies of the first excited states in the two-valence-neutron and -proton nuclei. The energy gap between the ground and first  $2^+$  states in  $^{134}\text{Sn}$  and  $^{210}\text{Pb}$  is in fact about 500 keV smaller than that in  $^{134}\text{Te}$  and  $^{210}\text{Po}$ , evidencing a reduction of the neutron pairing with respect to the proton one. As emphasized in Ref. [30], our shell-model study accounts for the close resemblance between the nuclei of each of these two pairs as well as for the difference between the two-valence-neutron and -proton nuclei.

As regards the effects of components with the pair coupled to  $J \neq 0$ , we have verified that their presence tends to produce

staggering with phase opposite to that observed in one proton-one neutron systems. This is evident for  $^{136}\text{Sb}$  but not for  $^{212}\text{Bi}$ . The explanation lies in the fact that in  $^{212}\text{Bi}$  this effect is quenched by configuration mixing, which we have found to be more relevant for this nucleus. As regards  $^{136}\text{I}$  and  $^{212}\text{At}$ , we don't find evidence of significant staggering, the curves of Fig. 2 being almost flat but for the lowest angular momenta. This is because, as mentioned above, the wave functions of the considered states in these nuclei contain a small percentage of nonzero-coupled proton pair components, giving rise to a staggering that is largely washed out by the configuration mixing.

In summary, we have performed here a comparative shell-model study of proton-neutron multiplets in  $^{132}\text{Sn}$  and  $^{208}\text{Pb}$  regions, focusing on the three far from stability nuclei  $^{134}\text{Sb}$ ,  $^{136}\text{I}$ ,  $^{136}\text{Sb}$  and their counterparts around stable  $^{208}\text{Pb}$ . We have shown that the calculated energies are in very good agreement with the available experimental data for all the six nuclei considered and emphasized that a close resemblance between the spectroscopy of the two regions persists when moving away from one proton-one neutron systems. A main achievement of our work is that this similarity emerges quite naturally from our shell-model interactions that are derived from a realistic  $NN$  potential without any adjustable parameters.

We are confident that this work may stimulate new experiments in both  $^{132}\text{Sn}$  and  $^{208}\text{Pb}$  regions and be a guide to the interpretation of data.

TABLE II. Diagonal matrix elements of  $V_{\text{low-k}}$  and  $V_{1p1h}$  (in MeV) for proton-proton and neutron-neutron configurations in  $^{132}\text{Sn}$  and  $^{208}\text{Pb}$  regions.

$J^\pi$	$(\pi 0g_{7/2})^2$		$(\pi 0h_{9/2})^2$		$(\nu 1f_{7/2})^2$		$(\nu 1g_{9/2})^2$	
	$V_{\text{low-k}}$	$V_{1p1h}$	$V_{\text{low-k}}$	$V_{1p1h}$	$V_{\text{low-k}}$	$V_{1p1h}$	$V_{\text{low-k}}$	$V_{1p1h}$
$0^+$	0.063	-0.549	0.079	-0.535	-0.403	-0.100	-0.227	-0.162
$2^+$	-0.016	0.071	-0.011	-0.013	-0.289	0.018	-0.226	-0.017
$4^+$	0.124	0.176	0.099	0.090	-0.136	0.051	-0.116	0.028
$6^+$	0.214	0.237	0.148	0.114	-0.063	0.067	-0.066	0.045
$8^+$			0.199	0.156			-0.029	0.058

- [1] J. Dobaczewski, N. Michel, W. Nazarewicz, M. Ploszajczak, and J. Rotureau, *Prog. Part. Nucl. Phys.* **59**, 432 (2007), and references therein.
- [2] H. Grawe, K. Langanke, and G. Martínez-Pinedo, *Rep. Prog. Phys.* **70**, 1525 (2007), and references therein.
- [3] T. Otsuka, T. Suzuki, and Y. Utsuno, *Nucl. Phys.* **A805**, 127c (2008), and references therein.
- [4] L. Coraggio, A. Covello, A. Gargano, and N. Itaco, *Phys. Rev. C* **73**, 031302(R) (2006).
- [5] J. Blomqvist, in *Proceedings of the 4th International Conference on Nuclei Far from Stability, Helsingor, Denmark, 7–13 June 1981*, CERN Report 81-09 (CERN, Geneva, 1981), p. 536.
- [6] G. A. Leander, J. Dudek, W. Nazarewicz, J. R. Nix, and Ph. Quentin, *Phys. Rev. C* **30**, 416(R) (1984).
- [7] C. T. Zhang *et al.*, *Phys. Rev. Lett.* **77**, 3743 (1996).
- [8] W. Urban *et al.*, *Eur. Phys. J. A* **5**, 239 (1999).
- [9] B. Fornal *et al.*, *Phys. Rev. C* **63**, 024322 (2001).
- [10] A. Korgul *et al.*, *Eur. Phys. J. A* **32**, 25 (2007).
- [11] V. I. Isakov *et al.*, *Phys. At. Nucl.* **70**, 818 (2007).
- [12] S. Sarkar and M. S. Sarkar, *Phys. Rev. C* **64**, 014312 (2001).
- [13] S. Sarkar and M. S. Sarkar, *Eur. Phys. J. A* **21**, 61 (2004).
- [14] J. Shergur *et al.*, *Phys. Rev. C* **71**, 064321 (2005).
- [15] E. K. Warburton and B. A. Brown, *Phys. Rev. C* **43**, 602 (1991).
- [16] G. H. Herling and T. T. S. Kuo, *Nucl. Phys.* **A181**, 113 (1972).
- [17] L. Coraggio, A. Covello, A. Gargano, and N. Itaco, *Phys. Rev. C* **72**, 057302 (2005).
- [18] A. Covello, L. Coraggio, A. Gargano, and N. Itaco, *Eur. Phys. J. ST* **150**, 93 (2007).
- [19] R. Machleidt, *Phys. Rev. C* **63**, 024001 (2001).
- [20] L. Coraggio, A. Covello, A. Gargano, and N. Itaco, *Phys. Rev. C* **76**, 061303(R) (2007).
- [21] S. Bogner, T. T. S. Kuo, L. Coraggio, A. Covello, and N. Itaco, *Phys. Rev. C* **65**, 051301(R) (2002).
- [22] L. Coraggio, A. Covello, A. Gargano, N. Itaco, and T. T. S. Kuo, *Prog. Part. Nucl. Phys.* **62**, 135 (2009), and references therein.
- [23] William D. M. Rae, *NUSHELLX for Linux* (Garsington, Oxford, 2007/2008); <http://knollhouse.org>.
- [24] J. R. Erskine, W. W. Buechner, and H. A. Enge, *Phys. Rev.* **128**, 720 (1962).
- [25] A. Korgul *et al.*, *Eur. Phys. J. A* **15**, 181 (2002).
- [26] Data extracted using the NNDC On-line Data Service from the ENSDF database, file revised as of 18 December 2008.
- [27] W. Urban *et al.*, *Eur. Phys. J. A* **27**, 257 (2006).
- [28] G. S. Simpson *et al.*, *Phys. Rev. C* **76**, 041303(R) (2007).
- [29] B. Fogelberg *et al.*, *Phys. Rev. C* **75**, 054308 (2007).
- [30] A. Covello, L. Coraggio, A. Gargano, and N. Itaco, *Acta Phys. Pol. B* **40**, 401 (2009).